Gastroenterology Report, 2024, **12**, goae045
https://doi.org/10.1093/gastro/goae045
Original Article

Original Article

ELMO1 ameliorates intestinal epithelial cellular senescence via SIRT1/p65 signaling in inflammatory bowel disease-related fibrosis

Junguo Chen[1,2,3,4,†], Guanman Li[1,2,3,5,†], Xiaowen He[1,†], Xijie Chen[1,6], Zexian Chen[1], Danling Liu[1], Shuang Guo[1], Tianze Huang[1], Yanyun Lin[1], Ping Lan[1,2,3], Lei Lian[6], Xiaosheng He[1,2,3,*]

[1]Department of General Surgery (Colorectal Surgery), The Sixth Affiliated Hospital,Sun Yat-sen University, Guangzhou, Guangdong, P. R. China
[2]Guangdong Provincial Key Laboratory of Colorectal and Pelvic Floor Diseases, The Sixth Affiliated Hospital, Sun Yat-sen University, Guangzhou, Guangdong, P. R. China
[3]Biomedical Innovation Center, The Sixth Affiliated Hospital, Sun Yat-sen University, Guangzhou, Guangdong, P. R. China
[4]Department of Thoracic Surgery, Thoracic Cancer Center, The Sixth Affiliated Hospital, Sun Yat-sen University, Guangzhou, Guangdong, P. R. China
[5]School of Medicine (Shenzhen), Sun Yat-sen University, Shenzhen, Guangdong, P. R. China
[6]Department of Gastrointestinal Surgery, The Sixth Affiliated Hospital of Sun Yat-sen University, Guangzhou, Guangdong, P. R. China

*Corresponding author. The Sixth Affiliated Hospital, Sun Yat-sen University, 26 Yuancun Erheng Road, Guangzhou, Guangdong 510655, China. Tel: +86-20-38254009; Email: hexsheng@mail.sysu.edu.cn

[†]These authors (J.G.C., G.M.L., and X.W.H.) have contributed equally to this work and share first authorship.

Abstract

Background: Intestinal fibrosis is a common complication in inflammatory bowel disease (IBD), which still lacks of reliable markers and therapeutic options. Cellular senescence has been considered an important mechanism of intestinal fibrosis, but the underlying molecular link remains elusive.

Methods: Tissues were stained using α-smooth muscle actin (α-SMA), fibronectin, and collagen I as markers of myofibroblastic differentiation. Cellular senescence was confirmed through Lamin B1 staining, senescence-associated β-galactosidase staining, and the expression of senescence-associated secretory phenotype (SASP) factors. We explored the relationship between senescence of intestinal epithelial cells (IECs) and intestinal fibrosis, as well as the molecular mechanism underlying this interaction. The effects of irisin on cellular senescence and fibrosis were determined.

Results: Here, we identify engulfment and cell motility protein 1 (ELMO1) as a novel biomarker for intestinal cellular senescence and fibrosis. In fibrostrictured tissues from patients and murine models with IBD, significantly high levels of cellular senescence score and factors were noted, which positively correlated with the fibrotic regulator fibronectin. Senescent IECs, not fibroblast itself, released SASP factors to regulate fibroblast activation. Prolonging exposure to severe and persistent injurious stimuli decreased ELMO1 expression, which dampened SIRT1 deacetylase activity, enhanced NF-κB (p65) acetylation, and thereby accelerated cellular senescence. Deletion of ELMO1 led to senescent IECs accumulation and triggered premature fibrosis in murine colitis. Furthermore, irisin, inhibiting the degradation of ELMO1, could downregulate p65 acetylation, reduce IECs senescence, and prevent incipient intestinal fibrosis in murine colitis models.

Conclusions: This study reveals ELMO1 downregulation is an early symbol of intestinal senescence and fibrosis, and the altered ELMO1-SIRT1-p65 pathway plays an important role in intestinal cellular senescence and IBD-related fibrosis.

Keywords: ELMO1; senescence; IBD-related fibrosis; p65 acetylation; irisin; exercise hormone

Introduction

Inflammatory bowel disease (IBD) is a chronic inflammatory gastrointestinal disorder, which affects 6.8 million people globally [1]. In China, the absolute number of hospitalized patients with IBD is estimated to reach 166,000 in 2018 [2]. Moreover, about one-third of patients with IBD develop a strictured disease phenotype during their lifetime [3]. Intestinal fibrosis is a long-term complication caused by persistent inflammation, recurrent injury, dysregulated tissue repair, and fibroblast proliferation and activation [4, 5]. Fibrotic remodeling in patients with IBD results in thickened muscularis propria, stricture formation, intestinal obstruction, and absorptive dysfunction [3]. Lacking of reliable predictive markers and effective therapies, patients with IBD suffer from this troublesome problem and finally require surgical intervention, which does not prevent disease recurrence or the development of fibrosis [6, 7]. Therefore, there is an urgent need for studies evaluating disease mechanisms and efficient methods for the prevention and reversal of intestinal fibrosis.

Received: 18 January 2024. **Revised:** 01 March 2024. **Accepted:** 10 April 2024

Although the specific mechanism of fibrosis in IBD remains unknown, it is widely accepted that the activation of cellular senescence enables mesenchymal cells (including fibroblasts, myofibroblasts, and smooth muscle cells) to acquire the ability to secrete collagens and fibronectins [8, 9]. Upon stimulation with senescence-associated secretory phenotype (SASP) factors released by senescent cells, fibroblasts are activated, start expressing α-SMA, and differentiate into myofibroblast-like cells [10]. An increasing number of studies have provided strong evidence that the treatment targeting senescence cells have shown promising effects in mitigating chronic diseases, such as pulmonary fibrosis and renal interstitial fibrosis [11–14]. Removal of senescent cells pharmacologically or genetically improves lung function and reverses pulmonary fibrosis induced by different stimuli in experimental fibrosis models [15]. Under maladaptive repair, premature senescent renal tubular cells can generate profibrotic factors that promote organ fibrosis [16]. These studies suggest that early attenuation of senescent cells is a promising therapeutic approach to prevent fibrosis. Sirtuin1 (SIRT1) plays a crucial role in regulating multiple cellular processes, including apoptosis, cellular senescence, and inflammation in mammals [17, 18]. SIRT1 protects against cellular senescence via regulating p53, the p65 subunit of nuclear factor-κB (NF-κB) and peroxisome proliferator-activated receptor-γ coactivator-1α (PGC-1α) [19]. Dysregulation of SIRT1 caused the accumulation of p53 and p65 acetylation, enhancing oxidative stress-induced cellular senescence [20]. Thus, enhancing SIRT1 deacetylase activity might be a visible approach for the amelioration of intestinal cellular senescence and fibrosis.

Evidence showed that prolonged healing could drive tissue damage and fibrogenesis in chronic inflammation [21]. Activated myofibroblasts and epithelial cells can be observed in wound healing. These cells undergo enhanced proliferation, migration, and differentiation to replace those dead or damaged cells during injury and lead to extracellular matrix production and deposition [22, 23]. Our earlier study found that engulfment and cell motility protein 1 (ELMO1) can promote epithelial wound healing via Rac1 activation in DSS-induced colitis murine models [24]. ELMO1 originally identified as orthologs of Caenorhabditis elegans CED-12 [25, 26], belongs to the engulfment and cell motility family which is a highly evolutionarily conserved protein family including ELMO1, ELMO2, and ELMO3 [25]. As its name implies, the family plays a crucial role in cytoskeleton rearrangements during phagocytosis, cellular migration, and chemotaxis [25]. As a key protein in this family, ELMO1 is involved in several inflammatory diseases, such as IBD, rheumatoid arthritis, kidney disease, and diabetic nephropathy [27–29]. In glioma cells, ELMO1 stimulated by IL-8 can initiate activation of the transcription factor NF-κB and increase the levels of matrix metalloprotease expression (MMP2 and MMP9), which exhibit a clear profibrotic role [30, 31]. However, the function of ELMO1 in IBD-related fibrosis and cellular senescence has not been addressed so far.

Cellular senescence has been considered an important mechanism of intestinal fibrosis, but the underlying molecular link remains elusive. We aim to explore the molecular mechanisms underlying cellular senescence and seek novel therapeutic targets for fibrosis linked to IBD. In this study, we present ELMO1 as a predictive factor for IBD-related fibrosis and explore its mechanisms and potential targets for treatment. Our study provides new insight into the role of ELMO1-SIRT1-p65 axis in regulating intestinal cellular senescence and fibrosis, thus suggesting that activation of this axis be a promising therapeutic strategy for IBD-related fibrosis in the future.

Materials and methods

Clinical samples

Clinical samples were provided by the Department of General Surgery (Colorectal Surgery), the Sixth Affiliated Hospital of Sun Yat-sen University (Guangzhou, Guangdong, China). CD patients with ileal fibrostrictured undergoing bowel resection were enrolled in this study. Normal, non-strictured and strictured tissues of the same patient ($n = 4$) were used for transcriptome-wide sequencing. Twenty inflamed colonic tissues (10 non-strictured and 10 strictured) were fixed in 10% phosphate-buffered formalin and embedded in paraffin for histological assessment. All participants provided signed informed consent. The study was approved by the Ethics Committee of Research involving human subjects at the Sixth Affiliated Hospital of Sun Yat-sen University (approval number: 2023ZSLYEC-367).

Animal experiments

C57BL/6 and *Elmo1*$^{-/-}$ (B6/JGpt-*Elmo1*$^{em1Cd/Gpt}$) mice were purchased from GemPharmatech and housed in rooms under controlled temperature (22°C–23°C) and 12-h light-dark cycle at the animal center in the Sixth Affiliated Hospital of Sun Yat-sen University. All mice with age- and sex-matched between 6 and 8 weeks of age were assigned randomly to groups.

The chronic colitis murine model was induced by three cycles of 7 days each, with a 2% (weight/volume) dextran sulfate sodium salt (DSS) (0216011080; MP Biomedicals; Heidelberg, Germany) in drinking water, followed by 2 weeks of tap water [32]. We used 2.5% 2,4,6-trinitro benzene sulfonic acid (TNBS; P2297; SIGMA; Karlsruhe, Germany) intrarectally after the initial abdominal challenge with 1% TNBS [32]. Six consecutive cycles were conducted. After the treatment, mice were euthanized by CO_2 inhalation. The colon was removed and its length and weight were measured. All animal studies were conducted in compliance with animal protocols approved by the Animal Care and Ethics Committee of Sun Yat-sen University and followed the National Health Guidelines on the Care and Use of Animals (IACUC-2022061701, IACUC-2022061702, and IACUC-2022061701).

Cell lines and incubation

The human intestinal epithelial cells HIEC6 (CRL-3266), human intestinal fibroblast cells CCD-18Co (CRL-1459), murine intestinal epithelial cells IEC6 (CRL-1592), murine intestinal fibroblast cells 3T3-L1 (CL-173) used in our study were purchased from the American Type Culture Collection (ATCC; Rockefeller, MD, USA) and cultured in DMEM-high glucose (C11995500BT; Gibco; Waltham, MA, USA) plus 10% fetal bovine serum (FBS; FSP500; ExCell Bio; Suzhou, Jiangsu, China) and 1% penicillin-streptomycin (15140–122; Gibco). Primary myofibroblasts (CP-H251) and primary intestinal epithelial cells (CP-H040) were obtained from Procell (Wuhan, Hubei, China). Myofibroblasts were isolated from the lamina propria and primary intestinal epithelial cells from the mucosa of normal ileum. All cell lines were incubated at 37°C and 5% CO_2 in a humidified atmosphere.

Transfection of shRNA

Based on the ELMO1 sequences (NM_080288.2), two shRNAs were designed and the sequences were as follows: sh*Elmo1*#1 (GCAGCTCCATGAACGAATACA); sh*Elmo1*#2 (GGAGATCACCATT GGCCAACT).

The *Elmo1* shRNA and scramble shRNA were purchased from GeneCopoeia. Cells were transfected with shRNA using ViraPower Lentiviral Packing Mix (L3000015; Invitrogen; Carlsbad, CA, USA) and 20 μL/mL polyethylenimine (PEI; 24314–2;

Polysciences; Warrington, PA, Polysciences) in Opti-MEM (31985062; Gibco). The lentiviruses were later co-cultured with intestinal epithelial cells (IECs) and fibroblasts to establish Elmo1 knock-down cell lines (sh*Elmo1*#1, sh*Elmo1*#2, and Scramble).

Drug treatment

For irisin (HY-P70664; MCE; NJ, USA) treatment, IEC6 cells were treated with 100 ng/mL irisin for 24 h. Conditioned medium (CM) was generated as follows: 1×10^6 *Elmo1*-knockdown and its control IEC6 cells were treated with or without 100 ng/mL irisin for 24 h, the culture medium was collected and harvested after cell debris was removed by filtering through 0.2-μM filters. To examine the effects of CM on fibroblasts, 3T3-L1 cells were separately treated with normal culture medium (Ctrl), CM from negative control IEC6 cells (CCM), CM from *Elmo1*-knockdown IEC6 cells (SCM), CM from DMSO treated *Elmo1*-knock down IEC6 cells (DCM), CM from irisin treated *Elmo1*-knockdown IEC6 cells (ICM), 2 ng/mL TGF-β and 100 ng/mL irisin. After culture for 2 days, cells were collected for further analysis.

Cell viability assay

Cell viability after drug treatment was assessed by CCK-8 kits (10,000 T; Dojindo; Kumamoto Prefecture, Kyushu Island, Japan) as previously described [33]. A total of 1×10^3 cells in the logarithmic growth phase were seeded into 96-well plates. Five duplicate wells were set for each group. After treatments, the culture medium was discarded. Then, 10 μL of the CCK-8 substrate was then added into each well with a total volume of 100 μL medium, the plates were incubated at 37°C for 3 h, and the OD values were measured with a spectrophotometer at a wavelength of 450 nm. CCK-8 assays were performed once a day until day 5. The growth curve was constructed by plotting absorbance against time.

Senescence-associated β-galactosidase staining

Senescence-associated β-galactosidase (SA-β-gal) staining was performed following the manufacturer's instructions (C0602; Beyotime; Shanghai, China). The frozen-section samples were received fresh from animal models, embedded in an optimal cutting temperature medium, and frozen using a cryostat at approximately −80°C. Subsequently, the frozen tissue was thawed and washed three times with phosphate buffered saline (PBS; C10010500BT; Gibco). Then, the sections were incubated overnight with freshly prepared staining solution at 37°C without CO_2 for 12 h. The SA-β-gal-stained intestinal epithelial cells were observed under a light microscope (Olympus IX71; Tokyo, Japan), and blue-stained cells represented senescent IECs.

RNA extraction and qPCR

The procedure was previously described [33]. Total RNA was extracted with Trizol reagent (15596018; Invitrogen). One microgram of total RNA was used for cDNA synthesis, using an RT-PCR kit (RR036A; Takara; Kusatsu, Shiga, Japan). The synthesized cDNA was then subjected to PCR using a SYBR Green PCR kit (04913914001; Roche; Basel, Switzerland) with primers. The amplification protocol consisted of incubations at 95°C for 15 s and 60°C for 60 s. GAPDH served as an endogenous control. All cycle threshold (CT) values were determined in real-time using CFX96™ Real-Time PCR Detection (Bio-rad; Hercules, CA, USA).

Fluorescence microscopy

Tissues (5 μm) were de-paraffinized in xylene and rehydrated with ethanol before antigen retrieval. After antigen retrieval in EDTA solution, the sections were washed with PBS for 15 min and treated with blocking buffer for 30 min at room temperature. For Lamin B1 staining, sections were incubated with anti-rabbit Lamin B1 antibody (1:200; AF5161-50; Affinity Biosciences; Melbourne, Australia) overnight at 4°C, and the fluorescently labeled secondary antibody (1:1000; coralite594, SA00013-4; Proteintech; Wuhan, Hubei, China) for 1 h at room temperature. For Lamin B1 and Fibronectin staining in cells, cells were seeded on glass slides and the slides were fixed in 4% formaldehyde in PBS for 15 min, washed three times in PBS, and then permeabilized with 0.1% TritonX-100 in PBS for 10 min. Slides were then blocked with 3% BSA in PBS for 1 h at room temperature followed by incubation with the primary antibody (Lamin B1, 1:200; Fibronectin, 1:200, 15613–1-AP, Proteintech) at 4°C overnight and the secondary antibody for 1 h at room temperature. Nuclei were stained with DAPI (HNFD-02; HelixGen). Images were taken with Olympus BX53 microscope.

Immunohistochemistry

Immunohistochemical staining was performed as described previously [33]. Mouse colon sections were de-paraffinized in xylene, rehydrated with ethanol, and incubated with 3% hydrogen peroxide to block endogenous peroxidase activity. For antigen retrieval, sections were heated in a microwave oven for 15 min in citrate buffer (pH 6.0). After being blocked with 20% goat serum (C-0005; Bioss; Beijing, China), sections were incubated at 4°C overnight with indicated primary antibodies. Subsequently, the EnVision Plus System-HRP (DAB; DAKO) was used according to the manufacturer's instructions, and counterstaining was performed using Mayer's hematoxylin. The percentage of the positive area or positive nuclei was quantified using ImageJ software (NIH).

Western blot analysis

Total cellular and nuclear proteins were extracted from cultured cells following the manufacturer's instructions (KGB5303-50; KeyGen Biotech; Nanjing, Jiangsu, China). The protein content was measured using the BCA Protein Assay Kit (KGP902; KeyGen Biotech). Equal amounts of protein were resolved on SDS–PAGE transferred onto a polyvinylidene fluoride membrane (PVDF; Merck Millipore; MA, USA), and then blocked with 5% skim milk for 1 h at room temperature. The membranes were incubated at 4°C overnight with different optimally diluted primary antibodies. Beta-tubulin or beta-actin were used as loading controls. This assay was performed in triplicate.

Statistical analysis

All data were conducted using commercially available software (SPSS version 22.0; Stanford University, USA). The association of ELMO1, p16, p21, TGF-β1, and PDGFα was determined using the Chi-square test or Fisher's exact test. Data from qPCR, cell viability, and western blot assays were evaluated using Student's *t*-test. Significance testing ($^*P < 0.05$, $^{**}P < 0.01$, $^{***}P < 0.001$) was performed as specified in the figure legends. Comparisons of multiple groups were analyzed by one-way ANOVA followed by *post hoc* Bonferroni correction. *P*-values < 0.05 were considered statistically significant. Unless otherwise indicated in the figure legends, all experimental results were based on six mice or human samples per group, and all experiments were repeated three times. Statistical tests were computed with GraphPad Prism (GraphPad Software; San Diego, CA, USA)

Results

Cellular senescence occurred in IBD-related fibrosis

To explore putative mechanisms in IBD-related fibrostrictured, we performed RNA-sequencing of four matched normal, strictured, and non-strictured colonic tissues from patients with IBD. The detailed workflow is shown in Supplementary Figure 1. A total of 2503 differentially expressed genes (DEGs) were detected in strictured tissues compared with non-strictured tissues (adjusted $P < 0.05$, Supplementary Figure 2A). Gene Ontology (GO) analysis of these DEGs indicated significant enrichment in terms of "cell aging" and "cellular senescence and aging" (Figure 1A). To assess the contribution of cellular senescence in IBD-related fibrostrictured, we compared the cellular senescence gene list (1,100 genes) from the CSGene database to our RNA-Seq data and generated a cellular senescence (CS) score (Supplementary Figure 2B–I) [34]. CS score is significantly increased in fibrostrictured tissues compared with adjacent normal tissues (Figure 1B and C). As the role of cellular senescence in intestinal fibrosis is still unclear, we examined the senescent biomarker Lamin B1 in patients with IBD. The reduction of Lamin B1 protein in the nucleus was considered a characteristic of senescence [35]. We found senescent cells with a decreased nuclear abundance of Lamin B1 were localized in the colonic epithelium in strictured IBD tissue specimens compared with IBD samples without strictured (Figure 1D). The mRNA levels of *p16*, *p21*, and SASP factors (including *IL-1β*, *IL-6*, *IL-8*, transforming growth factor *(TGF)-β*, platelet-derived growth factor *(PDGF)-α*, arginase *(ARG)-1*, and interferon *(IFN)-β)* were increased in the strictured tissue (Figure 1E). In both DSS and TNBS models, we confirmed histologic alterations of cellular senescence and fibrosis by qPCR assay, H&E, Masson's trichrome, fibronectin, SA-β-gal, and Lamin B1 staining. The results showed the factors of cellular senescence and fibrosis were upregulated in chronic murine colitis, which was consistent with our human results (Figure 1F and G). Taken together, these results suggested the correlation between intestinal senescence and intestinal fibrosis in chronic IBD.

Downregulation of ELMO1 was associated with cellular senescence and intestinal fibrosis

Better understanding the molecular mechanism of cellular senescence may discover new therapeutic targets for IBD-related fibrosis. Surprisingly, by conducting bioinformatics with our RNA-sequencing of human and murine intestinal fibrostrictured tissues, the result showed that ELMO1 was correlated both with cellular senescence and fibrosis (Supplementary Figure 3). In our previous study, ELMO1 is a key regulator of wound healing in IBD [24], but its function in cellular senescence and intestinal fibrosis remains unknown. Herein, we examined the *ELMO1* expression level in human and murine colonic tissues. The expression of *ELMO1* was significantly depressed and associated with lower CS score in strictured tissues (Figure 2A and B). By immunohistochemistry assay, we found the diminished infiltration of the Lamin B1 positive IECs in ELMO1-lowexpressed IBD tissues and revealed the negative correlation between senescent IECs infiltration and ELMO1 expression (Figure 2C and D). To further gain insight into ELMO1 expression in IBD-related fibrosis, mice were given TNBS or DSS treatment. Seven weeks after TNBS treatment or 10 weeks after DSS treatment, the mice developed a significant premature senescent phenotype, with reductions of Lamin B1, decreased ELMO1, and increased fibronectin in fibrostrictured colonic sections (Figure 2D and E). Of note, ELMO1 even started to decline 3 weeks after DSS or TNBS treatments (Figure 2F), indicating its downregulation was an early event in inflammation-triggered premature senescence *in vivo*. These data suggested that ELMO1 declined markedly along with the emergence of senescence in intestinal fibrostrictured.

Elmo1 deficiency accelerates senescence and aggravates intestinal fibrosis

To analyze the potential role of ELMO1 on fibrogenesis and senescence *in vivo*, we conducted experiments with *Elmo1*$^{-/-}$ mice. Subsequently, we attempted to investigate the relationship between senescence and fibrosis in TNBS/DSS models. In the chronic murine colitis, mucosal inflammation was exacerbated in mice deficient in *Elmo1*$^{-/-}$ mice compared to control mice, as observed by mini-endoscopy (Figure 3A). Correspondingly, the number of activated colonic fibroblasts was raised in *Elmo1*$^{-/-}$ mice, along with increased submucosal thickness and expression of fibrosis markers fibronectin (Figure 3B, C, and E). Accordingly, the levels of the SASP factors and cell-cycle regulator *p21* and *p16* were significantly increased in *Elmo1*$^{-/-}$ mice compared with wild-type controls (Figure 3D). The accumulation of senescent cells in strictured regions of *Elmo1*$^{-/-}$ mice was visualized using light-sheet fluorescence microscopy with SA-β-gal staining and Lamin B1 staining (Figure 3E). In addition, we observed that senescent cells were located in the intestinal epithelium (Figure 3E). Intriguingly, these data demonstrated that genetic inactivation of *Elmo1* resulted in markedly increased senescence and intestinal fibrosis in two different models of chronic colitis through putatively modulating the SASP pathways.

Elmo1-deletion-induced senescence in intestinal epithelial cells activates intestinal fibroblast

The above findings suggested that ELMO1 may be altered in the senescent process. To test this hypothesis, we examined endogenous ELMO1 expression in IECs (including IEC6 cell line, HIEC6 cell line, and primary IECs isolated from healthy volunteers called PIECs) upon LPS stimulation. IECs led to their senescence starting on day 3 and more notably on day 14, as measured by the induction of p21 (Figure 4A). Along with the emergence of senescence, ELMO1 protein declined markedly at day 14 (Figure 4A). LPS treatment could downregulate the staining of Lamin B1 and increase the expression of SASP factors (Figure 4B and C). To confirm whether senescent IECs can activate intestinal fibroblasts, we treated fibroblast (3T3-L1, CCD18-Co, and primary fibroblast isolated from healthy volunteer called PFC) with conditioned medium (CM) from senescent IECs (IEC6, HIEC6, and primary epithelial cells). TGF-β was used as a positive control for activated fibroblasts. We found that increased protein levels of collagen I, α-SMA, and fibronectin were detected in the ECM and LCM group (Figure 3C). Furthermore, the results showed that LPS could not induce senescence in fibroblasts (Figure 4A and Supplementary Figure 4).

To explore whether ELMO1 played a critical role in cellular senescence and fibrosis, we stably knocked down *ELMO1* in intestinal epithelial cells (IEC6, HIEC6, and PIEC cells) and fibroblast (3T3-L1, CCD18-Co and PFC cells) using two independent short hairpin RNAs (shRNAs; Figure 4B–D and Supplementary Figure 5). The ablation of *ELMO1* led to higher levels of *p21*, *p16*, and the SASP factors, as well as a reduction in the abundance of Lamin B1 in IECs (Figure 4E–G). Increased levels of collagen I, α-SMA, and fibronectin were detected in the SCM groups (Figure 4H).

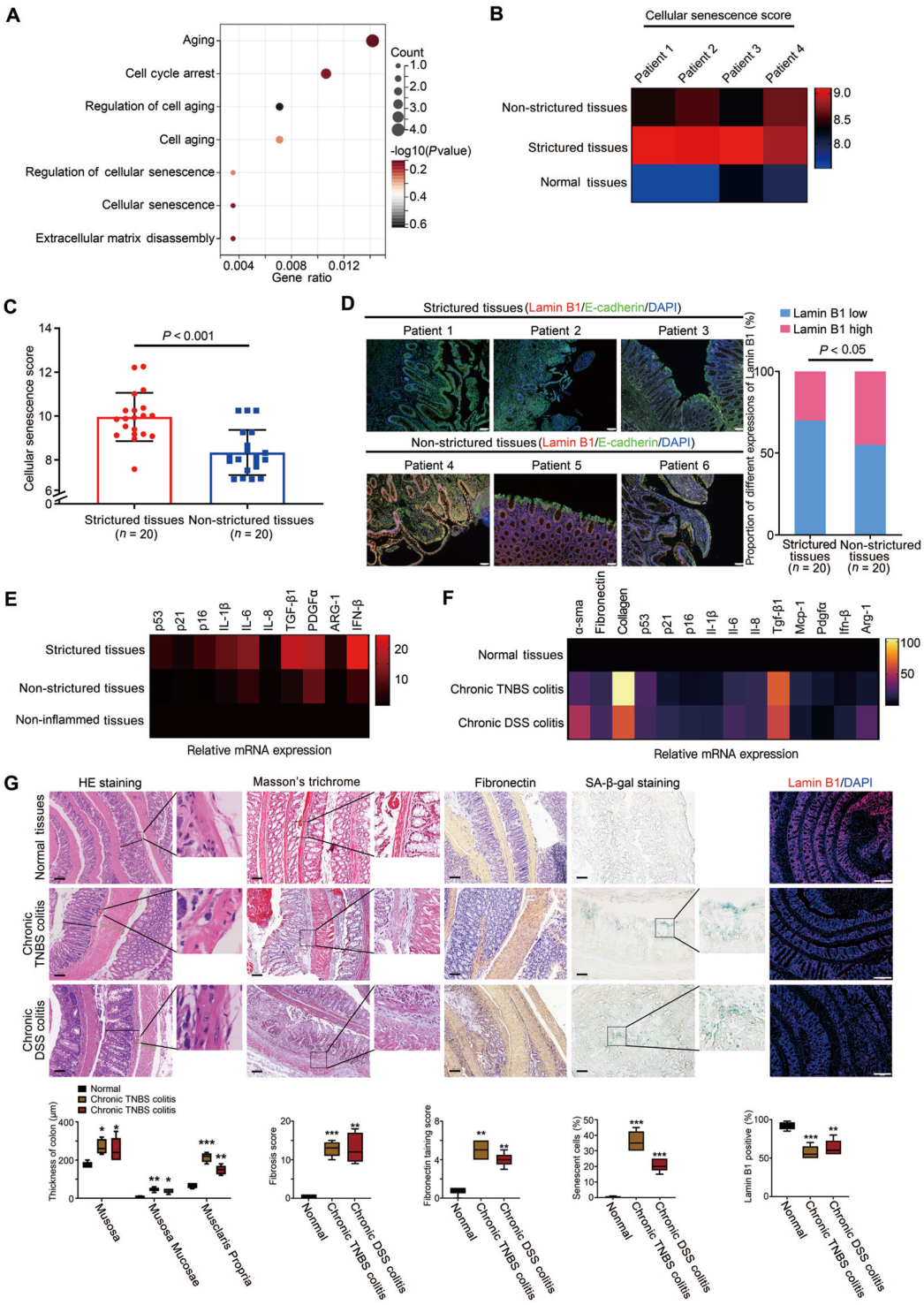

Figure 1. Intestinal fibrosis was associated with cellular senescence. (A) GO analysis of DEGs in four matched tissues from strictured and non-strictured patients with IBD. (B) Heat-map visualization of cellular senescence score in four matched tissues from strictured and non-strictured patients with IBD. (C) Histogram visualization of cellular senescence score based on the mRNA expression of colonic tissues from 40 patients with IBD. (D) Representative immunofluorescence image of Lamin B1 in the strictured and non-strictured tissue. Co-staining with Lamin B1, DAPI, and E-cadherin to identify senescent intestinal epithelial cells. scale bar: 100 μm. Binary classification of the correlation between LAMINB1 expression and fibrostrictured in IBD tissues. (E) qPCR assays were used to detect the mRNA expression of *p21*, *p16*, p53, and SASP genes in strictured, non-strictured, and non-inflamed tissue. (F) Relative mRNA expressions of *p53*, *p16*, and *p21* and SASP genes in chronic DSS or chronic TNBS models. (G) Distal colon tissue of unchallenged animals ($n = 5$), mice from chronic DSS ($n = 5$), and chronic TNBS colitis ($n = 5$) were stained with H&E, and the width of the submucosa was measured. (Scale bar: 100 μm) The thicknesses of the mucosa, submucosa, and muscularis were quantified ($n = 5$ per group, $^*P < 0.05$, $^{**}P < 0.01$, $^{***}P < 0.001$) from H&E staining of distal colon sections. Masson's Trichrome staining was performed in distal colon sections of unchallenged mice and animals from the chronic DSS or chronic TNBS models, respectively. Representative images of SA-β-gal staining (scale bar, 100 μm), immunofluorescence staining images of Lamin B1 (scale bar: 200 μm). Quantitative analyses were shown in the right panel. Values were reflected as the mean ± SD of three independent experiments. GO analysis = gene ontology analysis; DEGs = differentially expressed genes; IBD = inflammatory bowel disease; SASP = senescence-associated secretory phenotype; DSS = dextran sulfate sodium salt; TNBS = 2,4,6-trinitro benzene sulfonic acid; SA-β-gal = Senescence-associated β-galactosidase..

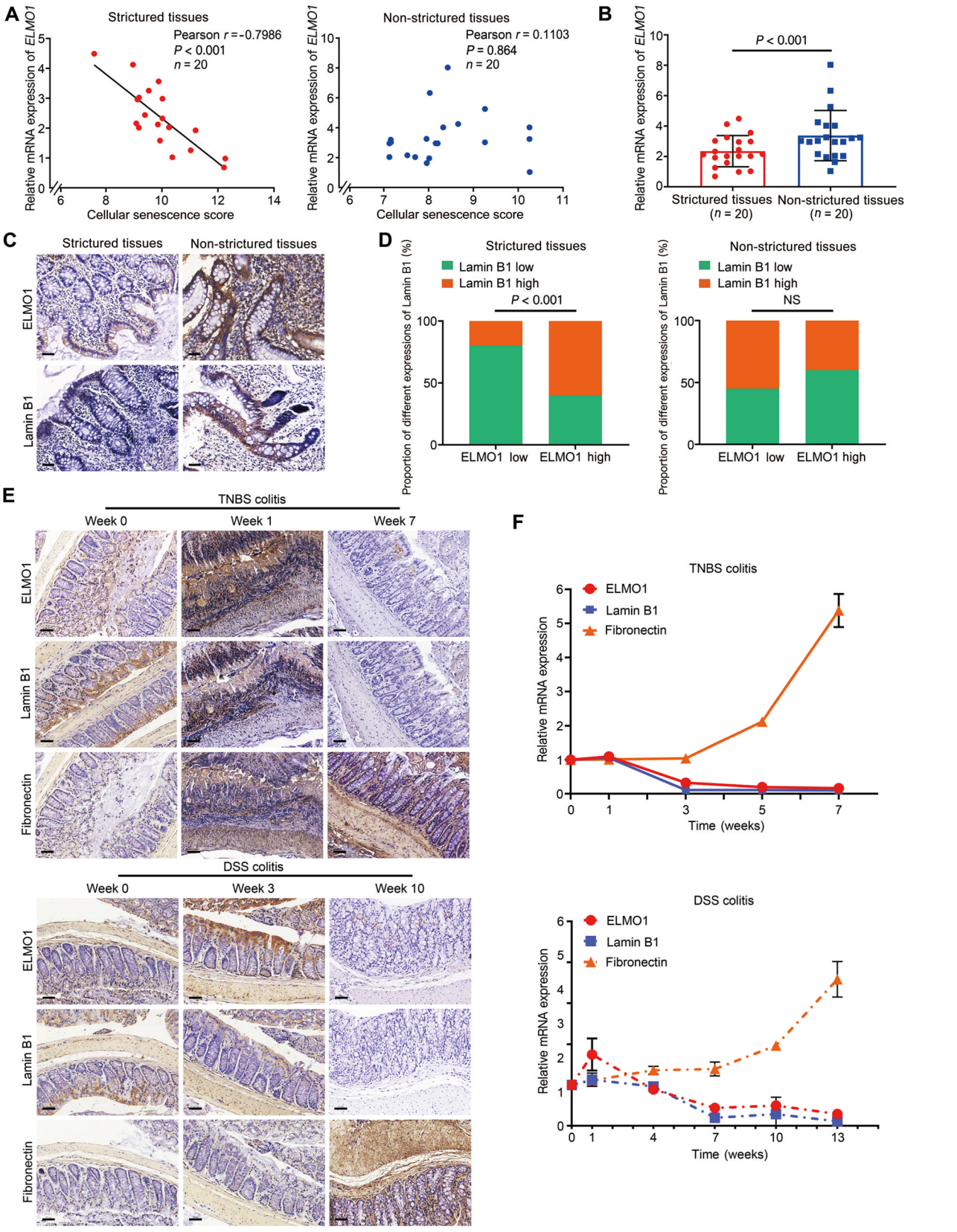

Figure 2. Downregulating ELMO1 was an early event in LPS-triggered cellular senescence and fibrostrictured. (A) The correlation between *ELMO1* expression and cellular senescence score in human strictured ($n = 20$) and non-strictured tissues ($n = 20$). (B) The expression of ELMO1 in human strictured and non-strictured tissues. (C) Immunohistochemical staining of ELMO1 and Lamin B1 in human strictured and non-strictured tissues. (D) Binary classification of the correlation between ELMO1 expression and the number of senescent cells in human strictured and non-strictured tissues. (E) Immunohistochemical staining of ELMO1, Lamin B1, and fibronectin in normal, early, and advanced stage of murine colitis models. (F) The mRNA expression of ELMO1 in normal, early, and advanced period of murine colitis models. NS = no significance.

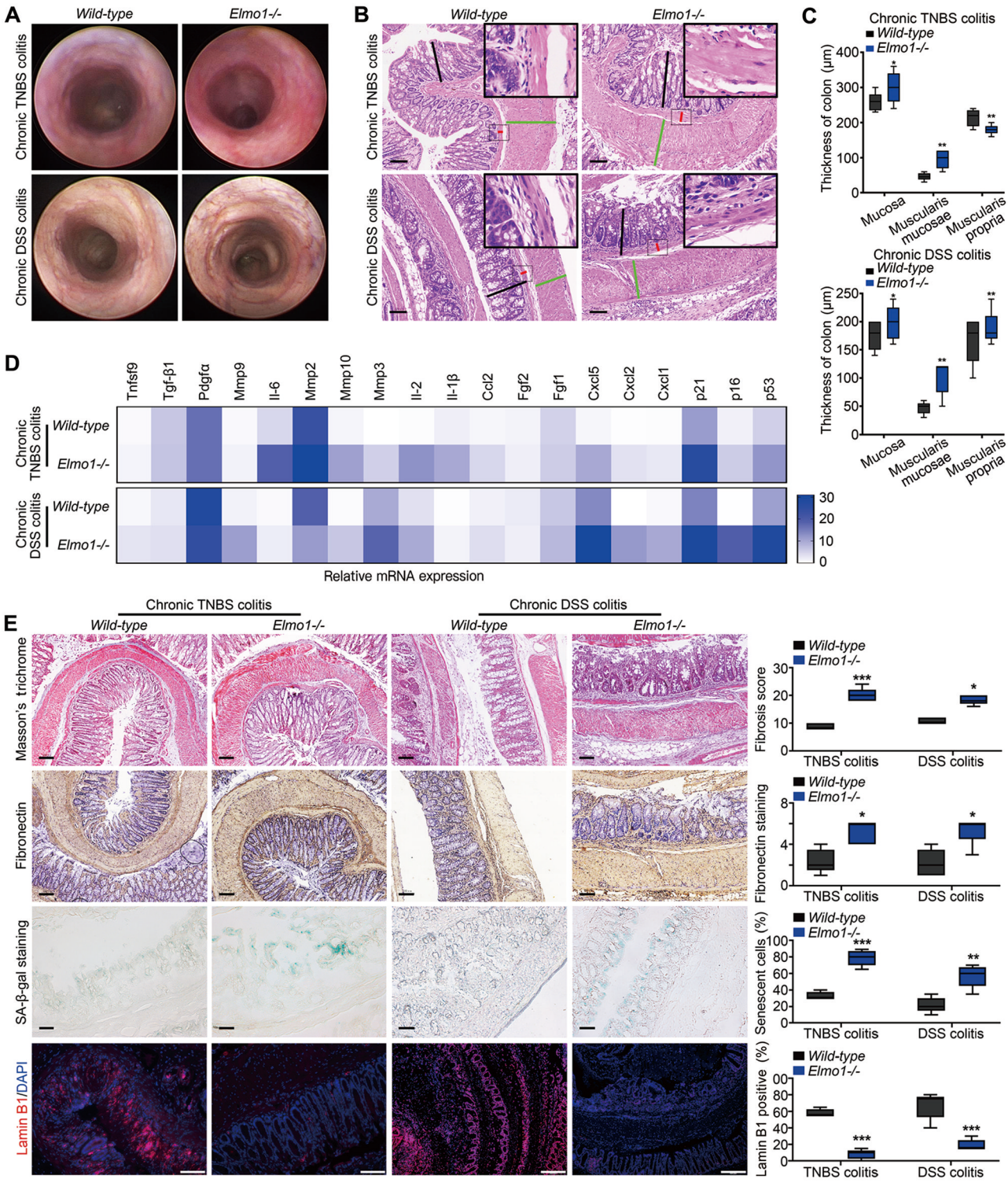

Figure 3. *Elmo1* deficiency causes severe fibrosis and is associated with epithelial cellular senescence in chronic murine colitis models. (A, B) Chronic TNBS or DSS colitis models were performed in *Elmo1*$^{-/-}$ mice or controls, and colon tissue was analyzed by mini-endoscopy[A] and H&E staining[B]. (C) The absolute thickness of the mucosa was measured in *Elmo1*$^{-/-}$($n = 5$) and wild-type colitis mice ($n = 5$) (D) Relative mRNA expressions of *p21*, *p16*, *p53*, and SASP genes in *Elmo1*$^{-/-}$ and wild-type colitis mice ($n = 5$). (E) Masson's trichrome staining, fibronectin staining, SA-β-gal staining, and Lamin B1 staining was measured in *Elmo1*$^{-/-}$ and wild-type colitis mice. (scale bar: 100 μm; *$P < 0.05$, **$P < 0.01$, ***$P < 0.001$). DSS = dextran sulfate sodium salt; TNBS = 2,4,6-trinitro benzene sulfonic acid; SASP = senescence-associated secretory phenotype; SA-β-gal = Senescence-associated β-galactosidase.

Immunofluorescence staining of fibronectin confirmed the activation of fibroblast by SCM (Figure 4I). However, the results showed that *Elmo1* deficiency could not activate fibroblasts and the mRNA level of *p21*, *p16*, and the SASP factors remained unaltered in *Elmo1*-ablated 3T3-L1 cells compared with its control group (Supplementary Figure 6). In summary, we concluded that

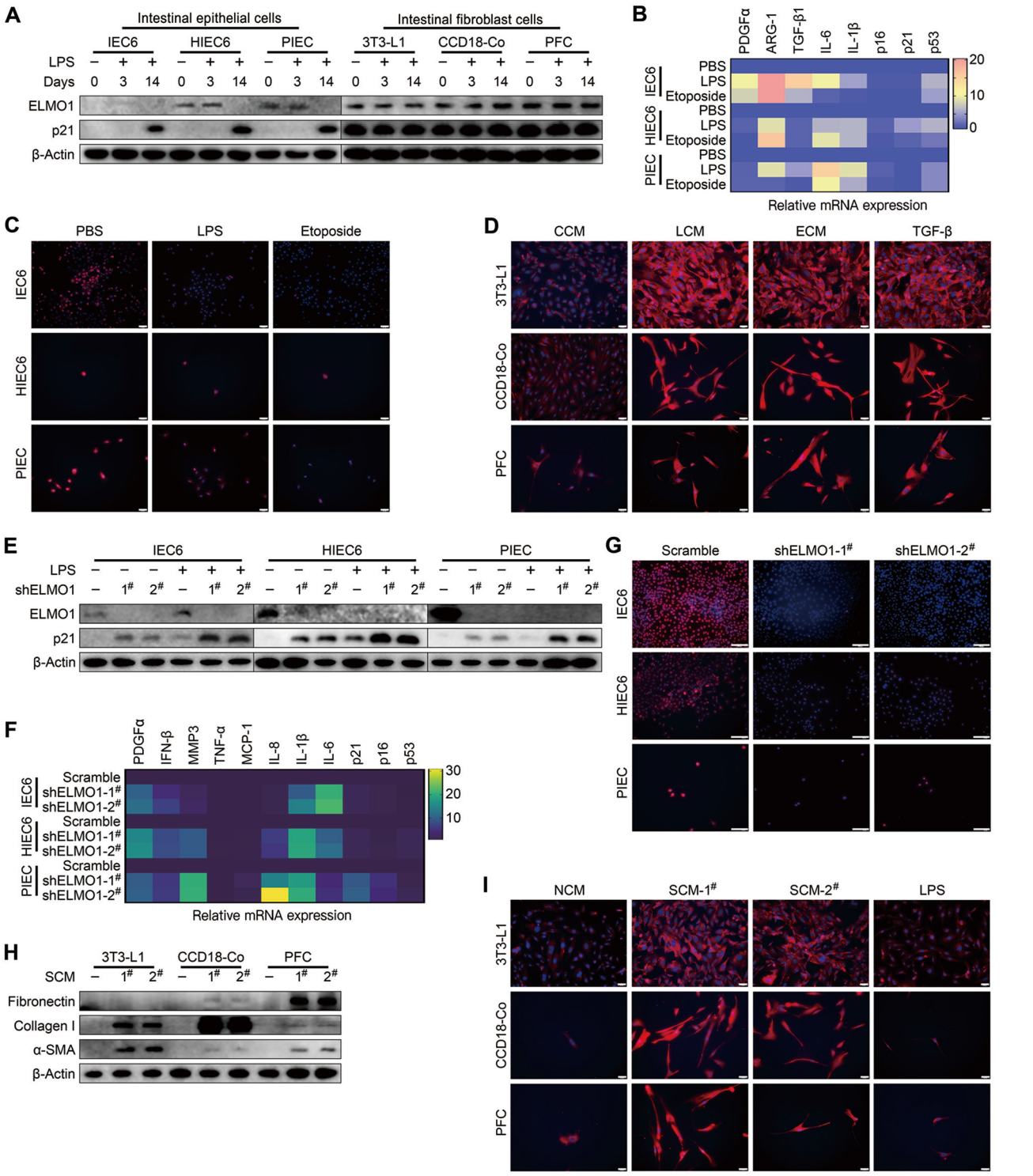

Figure 4. *Elmo1* deletion promotes senescence in IECs and activates fibrosis in fibroblasts. (A)Western blotting was performed to detect endogenous ELMO1 expression and senescence in the indicated cells upon LPS stimulation. Cell lysates were immunoblotted with the indicated antibodies. β-actin was used as a loading control. (B, C) IECs including IEC6, HIEC6, and primary epithelial cells were treated with or without 10 μM etoposide, 100 ng/mL LPS and PBS for 14 days. We used the etoposide as a positive control to induce senescence in IECs. Senescence activity was detected by qRCR assay (B) and Lamin B1 staining (C). (scale bar: 50 μm) (D) Fibroblasts were treated with conditioned media from normal epithelial cells (CCM), conditioned media from etoposide-induced epithelial cells (ECM), conditioned media from LPS-induced epithelial cells (LCM), and 2 ng/mL of TGF-β. TGF-β was used as a positive control for activated fibroblasts. Representative immunofluorescence images of fibronectin. (scale bar: 50 μm) (E–G) IECs including IEC6, HIEC6, and primary epithelial cells (PIEC) were transfected with sh-*ELMO1* plasmids and these groups were designed to exclude the effects of ELMO1 on senescence. Senescence activity was detected by western blotting (E), QRCR assay (F), and Lamin B1 staining (G) in *ELMO1*-silenced and scrambled cells. (H–I) Fibroblasts were treated with conditioned media from *ELMO1*-KD epithelial cells (SCM#1, SCM#2), conditioned media from normal epithelial cells (CCM), and 2 ng/mL TGF-β1. Western blotting was performed to detect the markers of intestinal fibrosis (H). Representative immunofluorescence images of fibronectin (I) (scale bar: 50 μm). LPS = lipopolysaccharides; IECs = intestinal epithelial cells; IEC6 = murine intestinal epithelial cells; HIEC6 = human intestinal epithelial cells; TGF-β = transforming growth factor-β; PIEC = primary epithelial cells; CCM = conditioned media from normal epithelial cells.

Elmo1-deletion-induced senescence could stimulate the transformation of fibroblasts to myofibroblasts, which was a hallmark of intestinal fibrosis.

Downregulation of ELMO1 attenuates SIRT1 deacetylase activity

Previous studies have revealed that upregulation of p21 and SASP genes indicated the activation of p53 and NF-κB pathways [36, 37]. RNA-seq data showed that PI3K-AKT signaling, MAPK signaling, p53 signaling, NF-κB signaling, and longevity regulation pathways were associated with chronic colitis mice tissue (Figure 5A). Based on the RNA-seq results and previous studies, we measured the expression of p53 and RelA/p65, a key transcription factor in the NF-κB pathway, in *Elmo1*-ablated IECs. The results showed a significant increase in the acetylation of p65 at lysine 310, while there were no alterations in p53-Lys382, total p53 protein levels, and p65 protein levels in three independent experiments (Figure 5B). As p300/CBP and histone deacetylase SIRT1 were reported to modulate the acetylation of p65, we also measured the expression of p300, CBP, and SIRT1 by western blot. Protein levels of p300 and CBP did not change significantly in *ELMO1*-depleted IECs, whereas SIRT1 protein was profoundly suppressed (Figure 5B). Additionally, nuclear SIRT activity markedly declined in *ELMO1*-depleted IECs (Figure 5C). Consistent with the acetylation of p65, the expression of IL-1β and IL-6 was upregulated in *Elmo1*-silenced IECs, suggesting that the activation of p65 via increased acetylation contributes to the cell-cycle arrest and SASP induced by *Elmo1* deletion (Figure 5D). Taken together, these observations suggested that the ELMO1-SIRT1 axis mediates the acetylation and activation of p65, which is pivotal for *Elmo1*-deletion-induced senescence.

Elmo1-deletion-induced senescence can be eliminated by irisin treatment

Since ELMO1 was reported to be a tumor promoter in colorectal cancer, we sought to evaluate the therapeutic potential of ELMO1-deletion-induced senescence and fibrosis. We observed that the key genes of longevity regulation pathway (including *Prkaa1* also named *Ampkα*, *Sirt1*, *Fndc5*, and *Ppargc1* also named *Pgc-1*) were downregulated in *Elmo1*$^{-/-}$ colitis colonic tissues (Supplementary Figure 7A). The results showed that the elevated acetylation of p65 on lys310 was abrogated under treatment with FNDC5 purified protein (Irisin; Figures 5E). Further examinations showed other agonists of SIRT1 or p65 did not significantly change the level of p65 acetylation, p21, p16, and SASP factors in ELMO1-silenced ICEs (Figure 5F, G, and Supplementary Figures 7B). Irisin, also known as a senolytic, could enhance longevity by boosting SIRT1 and AMPK activities [38]. After adding irisin to LPS-treated IECs, we found that the proportion of senescent IECs was decreased by almost 80% compared to senescent cells only treated by PBS (Figure 5H).

Based on the *in vitro* data and to explore whether intestinal fibrosis could be ameliorated by irisin treatment, we next analyzed the effect of irisin treatment in PFC cells. The culture media was collected to stimuli fibroblast. The mRNA levels of *α-SMA*, fibronectin, and collagen I were downregulated in the ISCM group (culture media from *Elmo1*-knockdown PIEC cells under irisin treatment; Figures 5I–K). Collectively, irisin treatment was able to reduce the burden of senescent cells induced by *Elmo1* deletion and diminished senescence-induced intestinal fibrosis.

Irisin treatment diminishes senescent cells and intestinal fibrosis in colitis murine model

To further investigate the potential of irisin in reducing intestinal senescence and fibrosis, we conducted experiments using a chronic TNBS model in wild-type and *Elmo1*$^{-/-}$ mice. We treated *wild-type* and *Elmo1*$^{-/-}$ mice with twice-a-week injections of irisin or saline at the same volume for 3 weeks (starting 3 weeks after the establishment of chronic TNBS colitis). Irisin treatment could reduce mucosal inflammation, decreased the mRNA expression of *p21*, *p16*, and SASP factors, and lowered the positive area of SA-β-gal staining in wild-type animals (Figure 6A–D). In the second approach, we analyzed fibrosis markers of the chronic TNBS model under irisin treatment. We measured less distorted crypt structures, diminished submucosal thickness, and decreased collagen accumulation (Figure 6E). Altogether, these data suggested that the essential effects of irisin on intestinal senescence and fibrosis were required for ELMO1 function in the chronic TNBS model.

Discussion

Here, we reported that ELMO1 functions as a gatekeeper of senescence-induced fibrosis in human and murine fibrostricture tissue. Persistent inflammatory injury dampened ELMO1-modulated SIRT1 deacetylase activity, increased p65 acetylation, and thereby promoted epithelial cells to undergo senescence. Senescent IECs regulated intestinal fibroblast activation and deteriorated tissue fibrosis through releasing SASP factors. Additionally, preventing the activation of the ELMO1-SIRT1-p65 axis by irisin treatment could abolish IECs senescence and intestinal fibrogenesis. Irisin could be a novel target molecule for the therapeutic approach to IBD-related fibrosis among ELMO1-downregulation patients.

The mechanisms by which cellular senescence drives tissue fibrosis remain unclear. In both chronic DSS and TNBS models, fibrosis was correlated with higher levels of senescent factors. Meanwhile, *Elmo1* deficiency caused an increase in collagen fibers, broader submucosal thickness, and higher levels of senescent genes in chronic colitis mice. Senescence is a stress response that elicits generally irreversible cell cycle arrest and triggers profound phenotypic changes to produce the pro-inflammatory microenvironment [39]. Inhibiting cell cycle progression causes the accumulation of senescent cells. For example, increased expression of p16 and p21 can inhibit the cell cycle, leading to cellular senescence [40, 41]. In this study, we observed an increased expression of p16 and p21 in two chronic colitis animal models, which was positively correlated with the downregulation of Elmo1 expression.

In IBD, IECs play a critical role in the repair and regeneration of bowel [42]. Prolonged exposure to severe and persistent injurious stimuli leads to maladaptive repair of IECs, characterized by persistent inflammation, an increase in mesenchymal cell numbers, and excessive extracellular matrix secretion. Then, fibrostrictured develops [6, 43, 44]. Maladaptive epithelial cells manifest an association between cell senescence and fibrosis [11, 45, 46]. In this study, silencing *ELMO1* in IECs shows strong induction of p21 but also shows elevated immunoreactivity for p16.

On the one hand, studies have shown that the BAI1/ELMO1/Rac1 signaling pathway contributes to the upregulation of ABCA1 in phagocytes as they engage apoptotic cells [47]. In vitro assay showed knockdown of *Elmo1* mediated lower level of cleaved caspase 3 in IEC6 cells. On the other hand, senescent cells are characterized by apoptosis resistance with upregulated anti-apoptotic proteins, particularly the Bcl-2 family proteins [48–53].

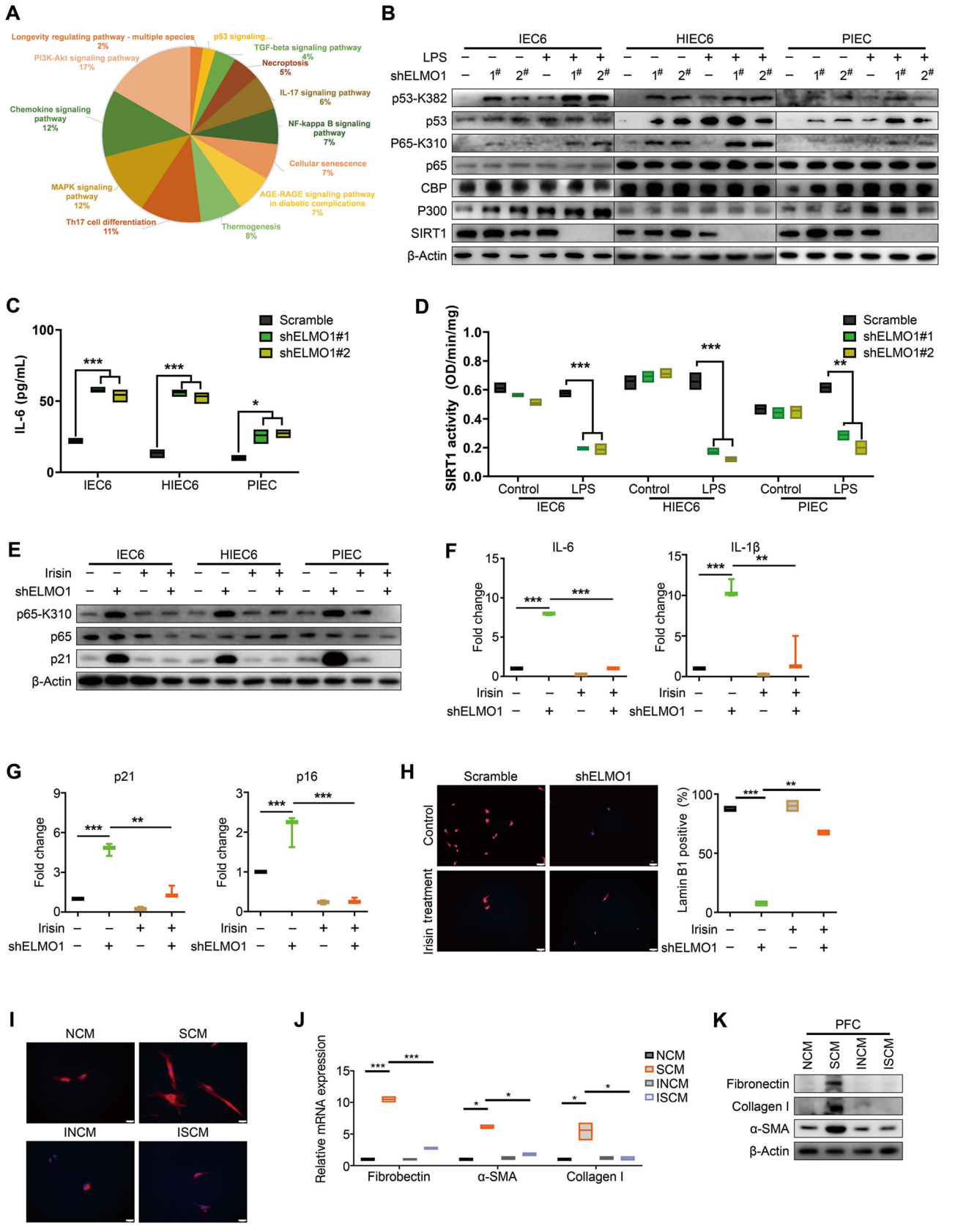

Figure 5. The declined SIRT1 deacetylase activity accounted for *Elmo1*-deletion-induced senescence. (A) RNA-sequencing was performed, and differentially expressed genes (fold change > 1.0, Benjamini-Hochberg corrected $P < 0.05$) were evaluated for pathways with Molecular Signatures Database hallmark gene sets. (B) Western blotting for p65, p65-K310 acetylation, p53, p53-K382 acetylation, p21, P300, CBP, and SIRT1 in *Elmo1*-silenced and its respective control cells under LPS treatment. (C) IL-6 protein concentration in the supernatants of *ELMO1*-KD cells co-cultured with control or 100 ng/mL LPS. (*$P < 0.05$, **$P < 0.01$, ***$P < 0.001$) (D) Knocking down ELMO1 suppressed the nuclear SIRT activity on days 0 and 14 upon LPS treatment. (E) The increased p65 acetylation upon ELMO1 depletion was blocked by irisin treatment. shCtrl- or shELMO1-transfected IECs were treated with 100 ng/mL irisin for 24 h and then subjected to immunoprecipitation. (F, G) Relative mRNA expressions of p21, *p16*, and SASP genes were detected in sh*Elmo1* and scramble cells under indicated treatments. (H) Representative immunofluorescence images of Lamin B1 (Scale bars: 100 μM). Senescent IECs were significantly decreased under irisin treatment. (I–K) Primary fibroblast cells (PFC) were separately treated with CM from scramble PIEC cells

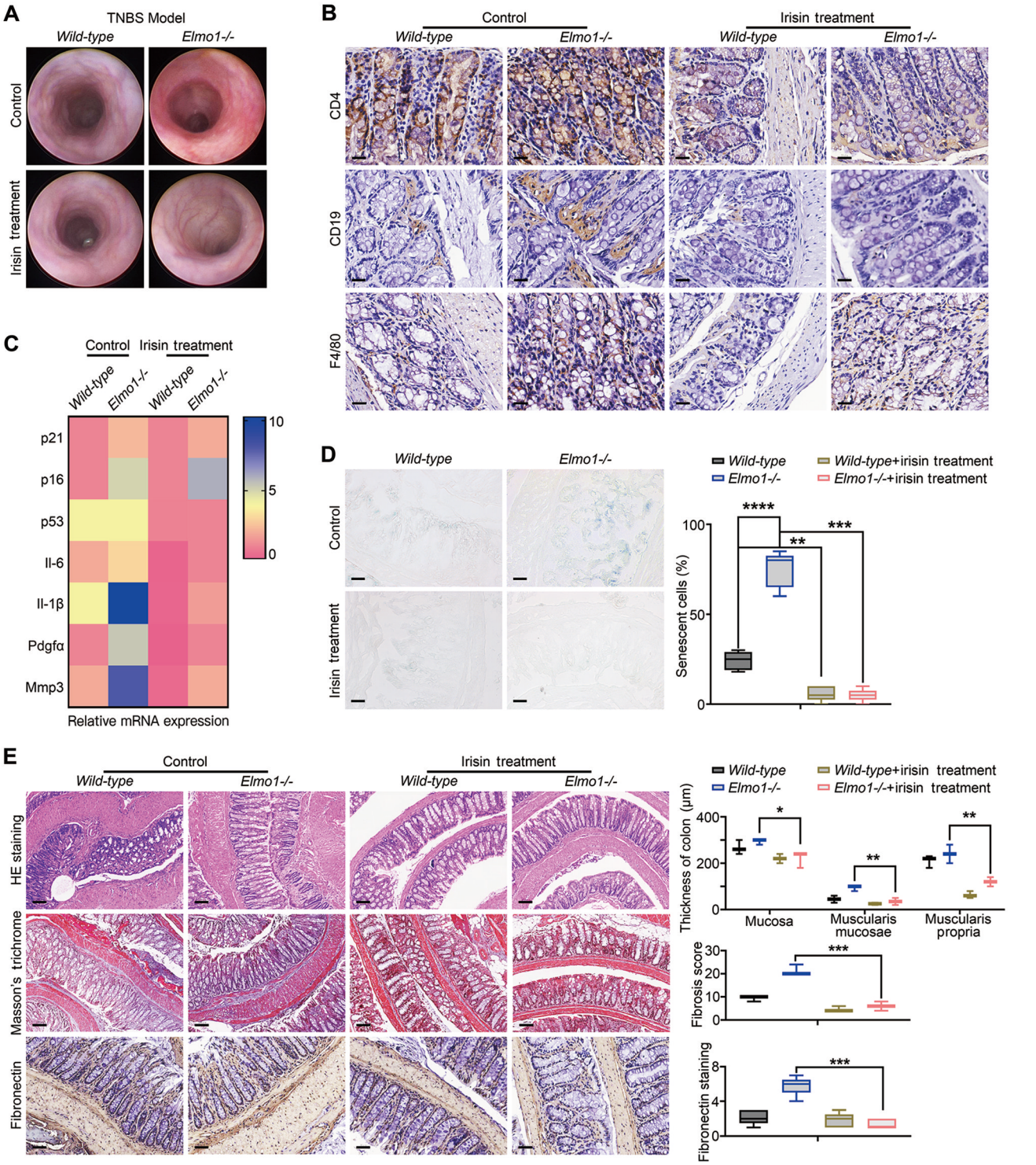

Figure 6. Irisin treatment ameliorates interstitial fibrosis in chronic colitis murine model. Animals were treated with twice-a-week injections of irisin or saline at the same volume for 3 weeks (starting 3 weeks after the establishment of chronic TNBS colitis). (A) Mucosal inflammation was analyzed in *Elmo1*$^{-/-}$ mice by mini-endoscopy. (B) IHC analysis of immune cell markers expressed on the colonic mucosa in chronic TNBS animals. (C) qPCR assay assessing the senescent regulators in chronic colitis mice with or without irisin injection. (D) SA-β-gal staining of the indicated colonic tissue in *Wild-type* and *Elmo1*$^{-/-}$ mice with chronic intestinal inflammation. Scale bar: 100 μm. (E) Colon samples from the experiments in A were stained with H&E, Masson's trichrome, and IHC staining. TNBS = 2,4,6-trinitro benzene sulfonic acid; IHC = Immunohistochemistry; qPCR = quantitative polymerase chain reaction; SA-β-gal = Senescence-associated β-galactosidase.

Figure 5. Continued
(CCM), CM from *ELMO1*-knockdown PIEC cells (SCM), CM from irisin treated scramble PIEC cells (DCM), CM from irisin treated *ELMO1*-knockdown PIEC cells (ISCM). (I) Representative immunofluorescence images of fibronectin (I) (Scale bars: 100 μM). (J) qPCR assay showing CM from irisin treated *ELMO1*-knockdown PIEC cells abrogated the fibroblast activation. (K) Western blotting assessing the fibrotic factors in PFC cells with ISCM. LPS = lipopolysaccharides; IECs = intestinal epithelial cells; PFC = primary fibroblast cells; PIEC = primary epithelial cells; CCM = conditioned media from normal epithelial cells; DCM = Conditioned medium from DMSO treated *Elmo1*-knock down IEC6 cells; ISCM = Conditioned medium from irisin treated *ELMO1*-knockdown PIEC cells;

We noticed that there was an increased level of Bcl-2 in *Elmo1*-silencing IECs and downregulating *Elmo1* rendered the cells resistant to apoptosis.

Although silencing *Elmo1* alone could not induce senescence in fibroblasts, the condition media collected from *Elmo1*-deficient IEC6 cells can trigger fibrogenic response in neighboring fibroblasts. Our data suggested that the knockdown of *Elmo1* can secret a complex mixture of pro-fibrotic factors to progress intestinal fibrosis. The SASP has been shown to play a critical role in senescence-associated fibrosis [54–61]. We observed the increased mRNA expression of SASP factors in *ELMO1*-deletion-induced senescent cells. Stimulating fibroblasts with CM from senescent *ELMO1*-depleted cells could activate fibroblasts into myofibroblasts *In vitro*. In two different chronic colitis mice models, the SASP factors were upregulated in *Elmo1*$^{-/-}$ colitis models, accompanied by increased levels of α-SMA, fibronectin, and collagen I. The components of the SASP attract and activate immune cells to remodeling the tissue environment aggravating intestinal inflammation.

There is a number of factors signal to induce the SASP such as cGAS-STING signaling [62], TLR4 signaling [63, 64], NF-κB signaling [36, 65], and et al. The acetylation of RelA/p65, a key transcription factor in NF-κB pathway, has been reported to enhance the transcriptional activity of SASP factors [36]. A recent study demonstrated that SIRT1 protects against oxidative stress-induced lung cellular senescence by increasing acetylation and activation of RelA/p65 as well as regulating the prosenescence gene p21 [66]. Quercetin is a stimulator of protein deacetylase SIRT1 interacting with Rel/p65 protein and specifically deacetylates lysine 310 [17, 67]. Quercetin has been shown to restore the susceptibility of senescent IPF fibroblasts to proapoptotic stimuli and mitigate bleomycin-induced pulmonary fibrosis in aged mice [68]. The research of Canto et al. supported that AMPK regulates energy expenditure by modulating NAD+ metabolism and SIRT1 activity [69]. Furthermore, activation of AMPK in key tissues can slow aging in a non-cell-autonomous manner [70]. Metformin, targeting AMPK/SIRT1/NF-κB pathway activation, could markedly reduce the SA-β-gal activity and the expression of p16, p21, and p53, indicating that the presence of metformin markedly inhibits oxidative stress-induced senescence [71, 72]. Our present study showed that silencing *ELMO1* in IEC6 suppressed the phosphorylation of AMPK on Thr172 and SIRT1 activity and elevated the acetylation of p65 on lys310. Besides, under quercetin or metformin treatment, *Elmo1*-deletion-induced senescence was eliminated with the activation of apoptotic protein, lower expression of SASP genes, and decreased level of *p21* and *p16*. Our finding identified ELMO1 as a cellular activator of AMPK and SIRT1.

Of note, we observed that inactivating AMPK by compound C significantly suppressed the expression of FNDC5, which is known as an exercise hormone that attenuates cognitive dysfunction in aging and Alzheimer's disease [73]. FNDC5 deficiency aggravates Ang II-induced oxidative stress and inflammasome activation and AMPK-SIRT1 activation is involved in the protective effects of FNDC5 on vascular oxidative stress and NLRP3 inflammasome activation [74]. In Wu's research, irisin could protect nucleus pulposus cells against senescence and apoptosis by activating autophagy [75]. Here, we found irisin treatment halted the proinflammatory SASP genes and *p16* and *p21* expression and ultimately eliminated *Elmo1*-deletion-incduced senescence and intestinal fibrosis both *in vivo* and *In vitro*. Irisin improved AMPK-T172 phosphorylation, enhanced SIRT1 deacetylase activity, and declined p65-K310 acetylation in *Elmo1*-silencing IEC6 cells, suggesting that this defined senescent pathway FNDC5-AMPK-SIRT1-p65 plays an irreplaceable role in *Elmo1*-deletion-induced senescence and fibrosis.

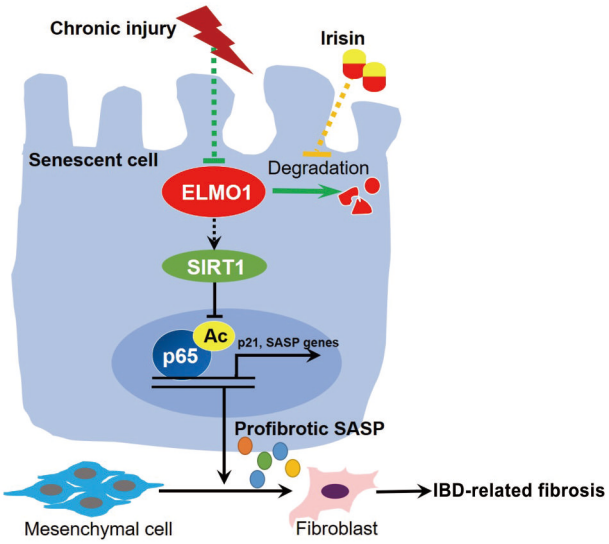

Figure 7. Schematic summary of our hypotheses and results. Cellular senescence is a new mechanism for IBD-related fibrosis. ELMO1 works as a gatekeeper for cellular senescence and intestinal fibrogenesis. Under chronic inflammation, ELMO1 loss impairs SIRT1 activity, increases p65 acetylation, and consequently induces epithelial cellular senescence and intestinal fibrosis. Inhibition of p65 acetylation by irisin treatment could reduce senescence and is an efficient therapy to prevent early-stage intestinal fibrosis in ELMO1-downregulated patients.

There are several limitations in our study. Firstly, although irisin can promote the secretion of ELMO1, further research is needed to investigate the direct interaction between ELMO1 and FNDC5. Secondly, the therapeutic effects of irisin have only been validated in the TNBS-induced chronic colitis model, and its efficacy in the DSS-induced chronic colitis model remains unknown. Thirdly, the therapeutic effects of irisin have only been studied in cellular and animal models, and human studies have not been conducted yet. This is the key areas of focus for our future attention.

In summary, our study demonstrated that ELMO1 protected against epithelial cellular senescence and played a crucial role in IBD-related fibrosis (Figure 7). Chronic injury suppressed ELMO1 expression. Downregulation of ELMO1 reduced SIRT1 activity, elevated p65 acetylation, and increased the expression of SASP factors, p21 and p16. Noteworthily, blocking p65 acetylation by irisin treatment significantly halted the SASP factors and ultimately ameliorated the IECs senescence and intestinal fibrosis in patients with ELMO1-downregulated IBD. Our findings suggested that ELMO1 downregulation might serve as a pro-fibrotic biomarker to predict IBD-associated fibrosis progression, and was of therapeutic benefit in mitigating IBD-related fibrosis.

Supplementary Data

Supplementary data is available at *Gastroenterology Report* online.

Authors' Contributions

J.G.C., G.M.L., and X.W.H. contributed equally to this work. G.M.L., J.G.C., and X.W.H. are the co-first authors. G.M.L., J.G.C., X.W.H., P.L., and X.S.H. conceived and designed the study; J.G.C., G.M.L. and X.W.H. performed *In vitro* experiments; G.M.L., J.G.C., Z.X.C., T.Z.H., Y.Y.L., D.L.L. and S.G. performed animal studies; J.G.C., G.M.L. and X.W.H. were involved in acquisition, analysis and

interpretation of data; J.G.C. and G.M.L. wrote and drafted the manuscript, P.L. and S.X.H. were involved in critical revision of the manuscript for important intellectual content; P.L., L.L. and S.X.H. supervised this study and provided funding. All authors approved the final version of the manuscript.

Funding

This work was supported by the National Natural Science Foundation of China [81970482 and 82172561], the Natural Science Foundation of Guangdong [2019A1515011313], the Guangdong Special Young Talent Plan of Scientific and Technological Innovation [2022B1515020022], the Complete Peeriod Talent Project of the Sixth Affiliated Hospital [R20210217202501976], the program of Guangdong Provincial Clinical Research Center for Digestive Diseases [2020B1111170004], the Guangzhou Science and Technology Plan Project [202201011160] and the National Key Clinical Discipline.

Conflicts of Interest

None declared.

References

1. GBDIBD Collaborators. The global, regional, and national burden of inflammatory bowel disease in 195 countries and territories, 1990-2017: a systematic analysis for the Global Burden of Disease Study 2017. *Lancet Gastroenterol Hepatol* 2020;**5**:17–30.
2. He YM, Mao R, Yuan G *et al.* The hospitalization burden of inflammatory bowel disease in China: a nationwide study from 2013 to 2018. *Therap Adv Gastroenterol* 2022;**15**:17562848221102307.
3. Rieder F, Fiocchi C, Rogler G. Mechanisms, management, and treatment of fibrosis in patients with inflammatory bowel diseases. *Gastroenterology* 2017;**152**:340–50 e6.
4. Henderson NC, Rieder F, Wynn TA. Fibrosis: from mechanisms to medicines. *Nature* 2020;**587**:555–66.
5. Yuan G, He Y, Cao QH *et al.* Visceral adipose volume is correlated with surgical tissue fibrosis in Crohn's disease of the small bowel. *Gastroenterol Rep (Oxf)* 2022;**10**:goac044.
6. Li J, Mao R, Kurada S *et al.* Pathogenesis of fibrostenosing Crohn's disease. *Transl Res* 2019;**209**:39–54.
7. Lenti MV, Di Sabatino A. Intestinal fibrosis. *Mol Aspects Med* 2019;**65**:100–9.
8. Ray D, Yung R. Immune senescence, epigenetics and autoimmunity. *Clin Immunol* 2018;**196**:59–63.
9. Huang W, Hickson LJ, Eirin A *et al.* Cellular senescence: the good, the bad and the unknown. *Nat Rev Nephrol* 2022;**18**:611–27.
10. Rieder F, Fiocchi C. Intestinal fibrosis in IBD—a dynamic, multifactorial process. *Nat Rev Gastroenterol Hepatol* 2009;**6**:228–35.
11. Li C, Shen Y, Huang L *et al.* Senolytic therapy ameliorates renal fibrosis postacute kidney injury by alleviating renal senescence. *Faseb J* 2021;**35**:e21229.
12. Justice JN, Nambiar AM, Tchkonia T *et al.* Senolytics in idiopathic pulmonary fibrosis: results from a first-in-human, open-label, pilot study. *EBioMedicine* 2019;**40**:554–63.
13. Roos CM, Zhang B, Palmer AK *et al.* Chronic senolytic treatment alleviates established vasomotor dysfunction in aged or atherosclerotic mice. *Aging Cell* 2016;**15**:973–7.
14. Zhang P, Kishimoto Y, Grammatikakis I *et al.* Senolytic therapy alleviates Abeta-associated oligodendrocyte progenitor cell senescence and cognitive deficits in an Alzheimer's disease model. *Nat Neurosci* 2019;**22**:719–28.
15. Yao C, Guan X, Carraro G *et al.* Senescence of alveolar type 2 cells drives progressive pulmonary fibrosis. *Am J Respir Crit Care Med* 2021;**203**:707–17.
16. Li C, Xie N, Li Y *et al.* N-acetylcysteine ameliorates cisplatin-induced renal senescence and renal interstitial fibrosis through sirtuin1 activation and p53 deacetylation. *Free Radic Biol Med* 2019;**130**:512–27.
17. Yeung F, Hoberg JE, Ramsey CS *et al.* Modulation of NF-kappaB-dependent transcription and cell survival by the SIRT1 deacetylase. *EMBO J* 2004;**23**:2369–80.
18. Chen J, Zhou Y, Mueller-Steiner S *et al.* SIRT1 protects against microglia-dependent amyloid-beta toxicity through inhibiting NF-kappaB signaling. *J Biol Chem* 2005;**280**:40364–74.
19. Hwang J-W, Yao H, Caito S *et al.* Redox regulation of SIRT1 in inflammation and cellular senescence. *Free Radic Biol Med* 2013;**61**:95–110.
20. Yan P, Li Z, Xiong J *et al.* LARP7 ameliorates cellular senescence and aging by allosterically enhancing SIRT1 deacetylase activity. *Cell Rep* 2021;**37**:110038.
21. Karin M, Clevers H. Reparative inflammation takes charge of tissue regeneration. *Nature* 2016;**529**:307–15.
22. Bankaitis ED, Ha A, Kuo CJ *et al.* Reserve stem cells in intestinal homeostasis and injury. *Gastroenterology* 2018;**155**:1348–61.
23. Hinz B. Myofibroblasts. *Exp Eye Res* 2016;**142**:56–70.
24. Zheng XB, Liu HS, Zhang LJ *et al.* Engulfment and cell motility protein 1 protects against dss-induced colonic injury in Mice via Rac1 activation. *J Crohns Colitis* 2019;**13**:100–14.
25. Gumienny TL, Brugnera E, Tosello-Trampont AC *et al.* CED-12/ELMO, a novel member of the CrkII/Dock180/Rac pathway, is required for phagocytosis and cell migration. *Cell* 2001;**107**:27–41.
26. Geisbrecht ER, Haralalka S, Swanson SK *et al.* Drosophila ELMO/CED-12 interacts with Myoblast city to direct myoblast fusion and ommatidial organization. *Dev Biol* 2008;**314**:137–49.
27. Parmar AS, Lappalainen M, Paavola-Sakki P *et al.* Association of celiac disease genes with inflammatory bowel disease in Finnish and Swedish patients. *Genes Immun* 2012;**13**:474–80.
28. Pezzolesi MG, Katavetin P, Kure M *et al.* Confirmation of genetic associations at ELMO1 in the GoKinD collection supports its role as a susceptibility gene in diabetic nephropathy. *Diabetes* 2009;**58**:2698–702.
29. Whitaker JW, Boyle DL, Bartok B *et al.* Integrative omics analysis of rheumatoid arthritis identifies non-obvious therapeutic targets. *PLoS One* 2015;**10**:e0124254.
30. Zhang B, Shi L, Lu S *et al.* Autocrine IL-8 promotes F-actin polymerization and mediate mesenchymal transition via ELMO1-NF-kappaB-Snail signaling in glioma. *Cancer Biol Ther* 2015;**16**:898–911.
31. Medeiros NI, Gomes JAS, Correa-Oliveira R. Synergic and antagonistic relationship between MMP-2 and MMP-9 with fibrosis and inflammation in Chagas' cardiomyopathy. *Parasite Immunol* 2017;**39**:e12446.
32. Wirtz S, Neufert C, Weigmann B *et al.* Chemically induced mouse models of intestinal inflammation. *Nat Protoc* 2007;**2**:541–6.
33. Li GM, Li L, Li MQ *et al.* DAPK3 inhibits gastric cancer progression via activation of ULK1-dependent autophagy. *Cell Death Differ* 2021;**28**:952–67.
34. Chatsirisupachai K, Palmer D, Ferreira S *et al.* A human tissue-specific transcriptomic analysis reveals a complex relationship between aging, cancer, and cellular senescence. *Aging Cell* 2019;**18**:e13041.
35. Freund A, Laberge RM, Demaria M *et al.* Lamin B1 loss is a senescence-associated biomarker. *Mol Biol Cell* 2012;**23**:2066–75.

36. Chien Y, Scuoppo C, Wang X *et al.* Control of the senescence-associated secretory phenotype by NF-kappaB promotes senescence and enhances chemosensitivity. *Genes Dev* 2011; **25**:2125–36.
37. el-Deiry WS, Tokino T, Velculescu VE *et al.* WAF1, a potential mediator of p53 tumor suppression. *Cell* 1993;**75**:817–25.
38. Sanchez B, Munoz-Pinto MF, Cano M. Irisin enhances longevity by boosting SIRT1, AMPK, autophagy and telomerase. *Expert Rev Mol Med* 2022;**25**:e4.
39. Birch J, Gil J. Senescence and the SASP: many therapeutic avenues. *Genes Dev* 2020;**34**:1565–76.
40. Ohtani N, Yamakoshi K, Takahashi A *et al.* The p16INK4a-RB pathway: molecular link between cellular senescence and tumor suppression. *J Med Invest* 2004;**51**:146–53.
41. Mijit M, Caracciolo V, Melillo A *et al.* Role of p53 in the regulation of cellular senescence. *Biomolecules* 2020;**10**:420.
42. Kurashima Y, Kiyono H. Mucosal ecological network of epithelium and immune cells for gut homeostasis and tissue healing. *Annu Rev Immunol* 2017;**35**:119–47.
43. Mack M. Inflammation and fibrosis. *Matrix Biol* 2018; **68-69**:106–21.
44. Prockop DJ. Inflammation, fibrosis, and modulation of the process by mesenchymal stem/stromal cells. *Matrix Biol* 2016; **51**:7–13.
45. Ferenbach DA, Bonventre JV. Mechanisms of maladaptive repair after AKI leading to accelerated kidney ageing and CKD. *Nat Rev Nephrol* 2015;**11**:264–76.
46. Zhang Y, Huang W, Zheng Z *et al.* Cigarette smoke-inactivated SIRT1 promotes autophagy-dependent senescence of alveolar epithelial type 2 cells to induce pulmonary fibrosis. *Free Radic Biol Med* 2021;**166**:116–27.
47. Fond AM, Lee CS, Schulman IG *et al.* Apoptotic cells trigger a membrane-initiated pathway to increase ABCA1. *J Clin Invest* 2015;**125**:2748–58.
48. He S, Sharpless NE. Senescence in health and disease. *Cell* 2017; **169**:1000–11.
49. Kale J, Osterlund EJ, Andrews DW. BCL-2 family proteins: changing partners in the dance towards death. *Cell Death Differ* 2018;**25**:65–80.
50. Lopez-Diazguerrero NE, Lopez-Araiza H, Conde-Perezprina JC *et al.* Bcl-2 protects against oxidative stress while inducing premature senescence. *Free Radic Biol Med* 2006;**40**:1161–9.
51. Tombor B, Rundell K, Oltvai ZN. Bcl-2 promotes premature senescence induced by oncogenic Ras. *Biochem Biophys Res Commun* 2003;**303**:800–7.
52. Wang E. Senescent human fibroblasts resist programmed cell death, and failure to suppress bcl2 is involved. *Cancer Res* 1995; **55**:2284–92.
53. Nelyudova A, Aksenov N, Pospelov V *et al.* By blocking apoptosis, Bcl-2 in p38-dependent manner promotes cell cycle arrest and accelerated senescence after DNA damage and serum withdrawal. *Cell Cycle* 2007;**6**:2171–7.
54. Wang WJ, Cai GY, Chen XM. Cellular senescence, senescence-associated secretory phenotype, and chronic kidney disease. *Oncotarget* 2017;**8**:64520–33.
55. Gorgoulis V, Adams PD, Alimonti A *et al.* Cellular senescence: defining a path forward. *Cell* 2019;**179**:813–27.
56. Morikawa M, Derynck R, Miyazono K. TGF-beta and the TGF-beta Family: Context-Dependent Roles in Cell and Tissue Physiology. *Cold Spring Harb Perspect Biol* 2016;**8**:a021873.
57. di Mola FF, Friess H, Scheuren A *et al.* Transforming growth factor-betas and their signaling receptors are coexpressed in Crohn's disease. *Ann Surg* 1999;**229**:67–75.
58. Shima H, Sasaki K, Suzuki T *et al.* A novel indole compound MA-35 attenuates renal fibrosis by inhibiting both TNF-alpha and TGF-beta(1) pathways. *Sci Rep* 2017;**7**:1884.
59. Wang JH, Su F, Wang S *et al.* CXCR6 deficiency attenuates pressure overload-induced monocytes migration and cardiac fibrosis through downregulating TNF-alpha-dependent MMP9 pathway. *Int J Clin Exp Pathol* 2014;**7**:6514–23.
60. Biancheri P, Pender SL, Ammoscato F *et al.* The role of interleukin 17 in Crohn's disease-associated intestinal fibrosis. *Fibrogenesis Tissue Repair* 2013;**6**:13.
61. Zhang HJ, Zhang YN, Zhou H *et al.* IL-17A promotes initiation and development of intestinal fibrosis through EMT. *Dig Dis Sci* 2018;**63**:2898–909.
62. Dou Z, Ghosh K, Vizioli MG *et al.* Cytoplasmic chromatin triggers inflammation in senescence and cancer. *Nature* 2017;**550**:402–6.
63. Hari P, Millar FR, Tarrats N *et al.* The innate immune sensor Toll-like receptor 2 controls the senescence-associated secretory phenotype. *Sci Adv* 2019;**5**:eaaw0254.
64. Davalos AR, Kawahara M, Malhotra GK *et al.* p53-dependent release of Alarmin HMGB1 is a central mediator of senescent phenotypes. *J Cell Biol* 2013;**201**:613–29.
65. Freund A, Patil CK, Campisi J. p38MAPK is a novel DNA damage response-independent regulator of the senescence-associated secretory phenotype. *EMBO J* 2011;**30**:1536–48.
66. Yao H, Chung S, Hwang JW *et al.* SIRT1 protects against emphysema via FOXO3-mediated reduction of premature senescence in mice. *J Clin Invest* 2012;**122**:2032–45.
67. Navarro-Nunez L, Lozano ML, Martinez C *et al.* Effect of quercetin on platelet spreading on collagen and fibrinogen and on multiple platelet kinases. *Fitoterapia* 2010;**81**:75–80.
68. Hohmann MS, Habiel DM, Coelho AL. Quercetin enhances ligand-induced apoptosis in senescent idiopathic pulmonary fibrosis fibroblasts and reduces lung fibrosis in vivo. *Am J Respir Cell Mol Biol* 2019;**60**:28–40.
69. Canto C, Gerhart-Hines Z, Feige JN *et al.* AMPK regulates energy expenditure by modulating NAD+ metabolism and SIRT1 activity. *Nature* 2009;**458**:1056–60.
70. Ulgherait M, Rana A, Rera M *et al.* AMPK modulates tissue and organismal aging in a non-cell-autonomous manner. *Cell Rep* 2014;**8**:1767–80.
71. Zheng Z, Bian Y, Zhang Y *et al.* Metformin activates AMPK/SIRT1/NF-kappaB pathway and induces mitochondrial dysfunction to drive caspase3/GSDME-mediated cancer cell pyroptosis. *Cell Cycle* 2020;**19**:1089–104.
72. Chen D, Xia D, Pan Z *et al.* Metformin protects against apoptosis and senescence in nucleus pulposus cells and ameliorates disc degeneration in vivo. *Cell Death Dis* 2016;**7**:e2441.
73. Islam MR, Valaris S, Young MF *et al.* Exercise hormone irisin is a critical regulator of cognitive function. *Nat Metab* 2021; **3**:1058–70.
74. Zhou B, Qiu Y, Wu N *et al.* FNDC5 attenuates oxidative stress and NLRP3 inflammasome activation in vascular smooth muscle cells via activating the AMPK-SIRT1 signal pathway. *Oxid Med Cell Longev* 2020;**2020**:6384803.
75. Zhou W, Shi Y, Wang H *et al.* Exercise-induced FNDC5/irisin protects nucleus pulposus cells against senescence and apoptosis by activating autophagy. *Exp Mol Med* 2022;**54**:1038–48.

Gastroenterology Report, 2024, 12, 1–14
https://doi.org/10.1093/gastro/goae045
Original Article